

Determination of HNO_3 dry deposition by modified Bowen ratio and aerodynamic profile techniques

By H. MÜLLER^{1*}, G. KRAMM¹, F. MEIXNER^{1**}, G. J. DOLLARD², D. FOWLER³, and M. POSSANZINI⁴, ¹Fraunhofer-Institut für Atmosphärische Umweltforschung (IFU), Kreuzteckbahnstraße 19, D-8100 Garmisch-Partenkirchen, Germany; ²Harwell Laboratory, Modelling and Assessments Group (AEA), Oxfordshire OX11 0RA, UK; ³Institute of Terrestrial Ecology (ITE), Bush Estate, Penicuik, Midlothian EH26 0QB, UK; ⁴Istituto sull'Inquinamento Atmosferico, Via Salaria Km., 29, 300, I-00016 Monterotondo Stazione (Roma), Italia

(Manuscript received 28 October 1991; in final form 15 March 1993)

ABSTRACT

Modified Bowen ratio and aerodynamic profile techniques based on the constant flux approach were utilized to derive the deposition fluxes and deposition velocities (v_d) of gaseous nitric acid from measurements made during two joint field experiments over low vegetation (grassland, LOVENOX, Halvergate, UK, September 1989) and over a wheat canopy (ecosystem wheat, Mandorf, Germany, July 1990). Both micrometeorological methods are discussed in more detail and in context with the flux-resistance analogy to provide a complete conceptual evaluation guide for HNO_3 dry deposition analysis. Daytime dry deposition of nitric acid was found to be fast with an average v_d of $2.2 \pm 1.2 \text{ cm s}^{-1}$ and a range of 0.6 to 5.0 cm s^{-1} . The derived deposition velocities are in broad agreement with estimates of other authors. The data have also been used to check sublayer Stanton numbers which are of basic importance in determining the viscous sublayer resistance yet not well quantified.

1. Introduction

It is well-established that dry deposition plays an important role in the atmospheric mass budget of many gaseous species. Especially in the vicinity of sources of pollution, dry deposition is often more important than wet deposition (cf. Businger, 1986).

Dry deposition removal from the atmosphere depends on the micrometeorological transfer properties of the atmospheric surface layer (often called the Prandtl layer), the capability of vegetation and soil to take up matter, and the prevailing chemical and photochemical environment (cf. Kramm, 1989a; Dlugi et al., 1989). Whereas the removal by wet deposition is a result of in-cloud

and below-cloud scavenging processes which are efficient across deep layers of the troposphere under quite different weather conditions. Since the origin of dry deposition differs from that of wet deposition, which is manifested in different compositions of chemical compounds and ions, it is necessary to separately investigate both deposition processes and their effects on vegetation, soil and water (see also Dlugi et al., 1989).

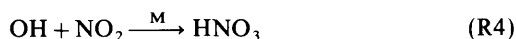
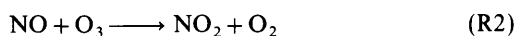
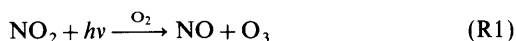
Nitrogen oxides, acidic and organic compounds play an important role in many air pollution problems including the formation of photochemical oxidants and acidification of the environment (see, e.g., Finlayson-Pitts and Pitts, 1986; Dollard et al., 1990). Nitric acid is a final product of the oxidation processes involved in the photochemical smog formation (see Ehhalt and Drummond, 1982) and is one of the most important nitrogen containing species. A typical evolution of the HNO_3 concentration near the surface ($\approx 1 \text{ m}$

* Corresponding author.

** Present affiliation: Max-Planck-Institut für Chemie, Abteilung Biogeochemie, D-6500 Mainz, Germany.

above a wheat canopy) is illustrated in Fig. 1. Based on 7 (one hour) runs, which are discussed later, a distinct increase of concentration becomes evident before noon. It almost coincides with the increase of the ozone concentration and closely follows the course of solar radiation and is an indication of the photochemical origin of nitric acid. Note that the rate of HNO₃ increase is of the same order as that observed by other authors on clear summer days (see, e.g., Cadle et al., 1982).

In the light of the photochemical origin of HNO₃, Bowen ratio and aerodynamic profile techniques (based on the constant flux approach and adopted in this study to derive HNO₃-fluxes) seem to be doubtful methods to provide reasonable flux results. However, model studies of Kramm et al. (1991) on the deposition fluxes of NO, NO₂, O₃, and HNO₃ including chemical reactions according to



indicate that in the absence of NH₃ the fluxes of HNO₃ are nearly constant with height (see Fig. 2), so that the constant flux approach appears to be appropriate in deriving HNO₃ dry deposition characteristics.

There are additional chemical processes which might violate the constant flux assumption. Besides the inorganic nighttime chemistry characterized by the NO₃-N₂O₅-HNO₃ cycle which has to be considered as an important source of nitric acid (see, e.g., McRae and Russell, 1984), but

which cannot be introduced in deposition estimations at present, the triad HNO₃-NH₃-NH₄NO₃ represents a strong interrelation between gaseous and particulate nitrogen containing compounds which may cause depletion and formation of nitric acid along with the formation and dissociation of ammonium nitrate.

The governing chemical reactions of this nitrous triad are given by (see Stelson and Seinfeld, 1982)



Unfortunately, neither the structure of these chemical reactions nor the reaction rate constants are well-known (see, e.g., Brost et al., 1988; Harrison et al., 1989). Therefore, Kramm and Dlugi (see Kramm, 1992), in an attempt to model vertical fluxes of this nitrous triad, recommend a (pseudo-)second order reaction for the formation of NH₄NO₃ (R5) with a reaction rate constant k_5 (expressed in units of ppm⁻¹ min⁻¹) and a first order reaction for the dissociation of NH₄NO₃ (R6) with a reaction rate constant k_6 (expressed in units of min⁻¹). This recommendation is in accordance with the time-invariance of total nitrate, TN = [HNO₃] + [NH₄NO₃], and total ammonia, TA = [NH₃] + [NH₄NO₃], which is used to determine the concentrations of HNO₃, NH₃, and NH₄NO₃ at equilibrium given by (see also Hildemann et al., 1984)

$$[\text{NH}_4\text{NO}_3]_{\text{eq}} = 1/2 \{ \text{TN} + \text{TA} - ((\text{TN} + \text{TA})^2 - 4(\text{TN} \text{TA} - k_p))^{1/2} \}, \quad (1)$$

$$[\text{HNO}_3]_{\text{eq}} = \text{TN} - [\text{NH}_4\text{NO}_3]_{\text{eq}}, \quad (2)$$

$$[\text{NH}_3]_{\text{eq}} = \text{TA} - [\text{NH}_4\text{NO}_3]_{\text{eq}}, \quad (3)$$

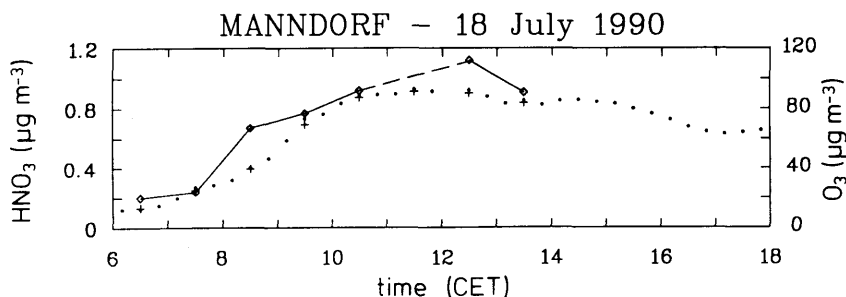


Fig. 1. Time variation of HNO₃ concentration at $z = 2$ m (\diamond : hourly means) and O₃ concentration at $z = 4.5$ m ($+$: hourly means, dots: 20 min means).

BIATEX-LOVENOX, Halvergate, 20-SEP-89, 14:40 - 17:20 GMT

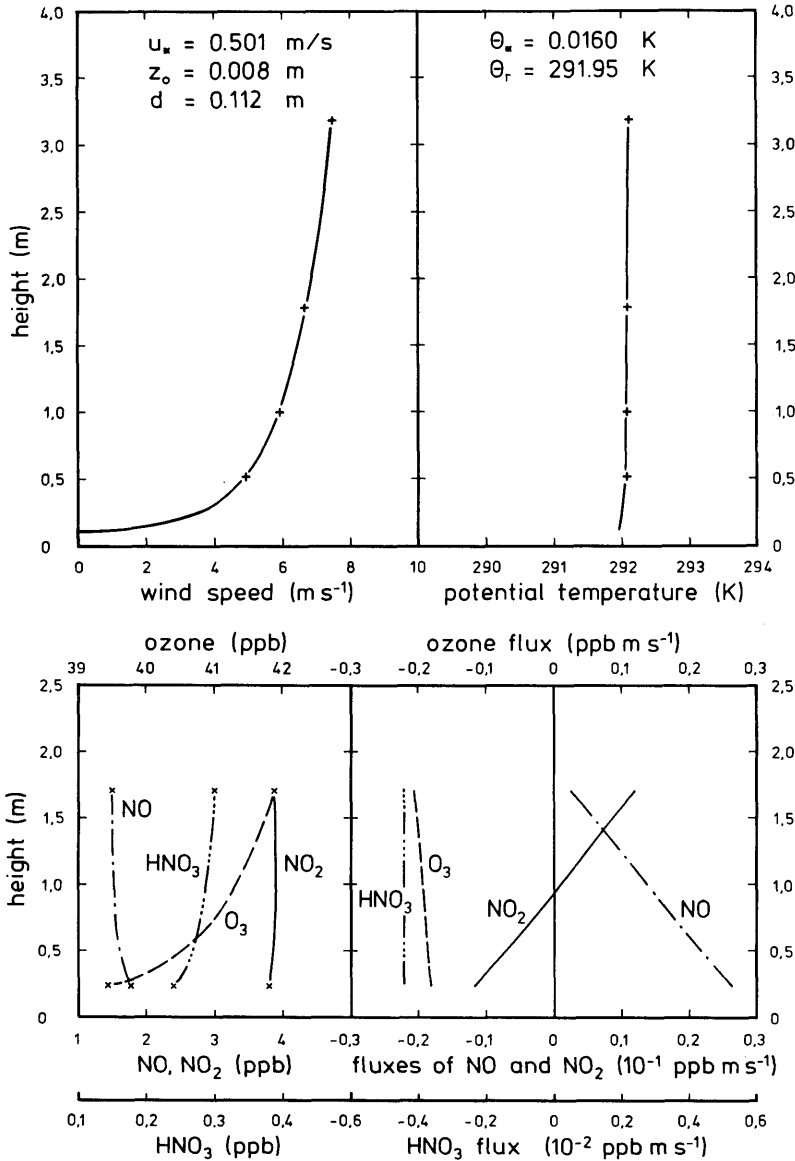


Fig. 2. Vertical profiles of wind velocity (U) and potential temperature (θ) as well as vertical profiles and fluxes of NO, NO₂, O₃, and HNO₃. The crosses represent observed values and the lines calculated profiles (from Kramm et al., 1991).

with k_p being the equilibrium dissociation constant of the nitrous triad for an ambient relative humidity less than the relative humidity of deliquescence (see Stelson and Seinfeld, 1982). Note, that the first order chemical relaxation preferred

and utilized by Brost et al. (1988) for modelling the vertical profiles of concentrations and fluxes of HNO₃, NH₃, and NH₄NO₃ violates the time-invariance of TN and TA (a prerequisite to determine the equilibrium concentrations which were,

on the other hand, used to formulate the first order relaxation approach; for details see Kramm, 1992).

The results shown in Figs. 3 and 4 are based on the same concentration values (at 20 m height) as used by Brost et al. (1988) and the same equilibrium constant (see Stelson and Seinfeld, 1982) rearranged to $k_p = (298/T)^{6.1} \exp(84.6 - 24,220/T)$ ppb². Since the mentioned reaction rate constants k_5 and k_6 are not well-

known, sensitivity studies with different values for k_5 and k_6 were performed, where the relationship (see Kramm, 1992)

$$\frac{k_6}{k_5} = \frac{k_p}{[\text{NH}_4\text{NO}_3]_{\text{eq}}} \quad (4)$$

was used. The results illustrate that for low values of k_5 all flux divergences are negligible and, hence,

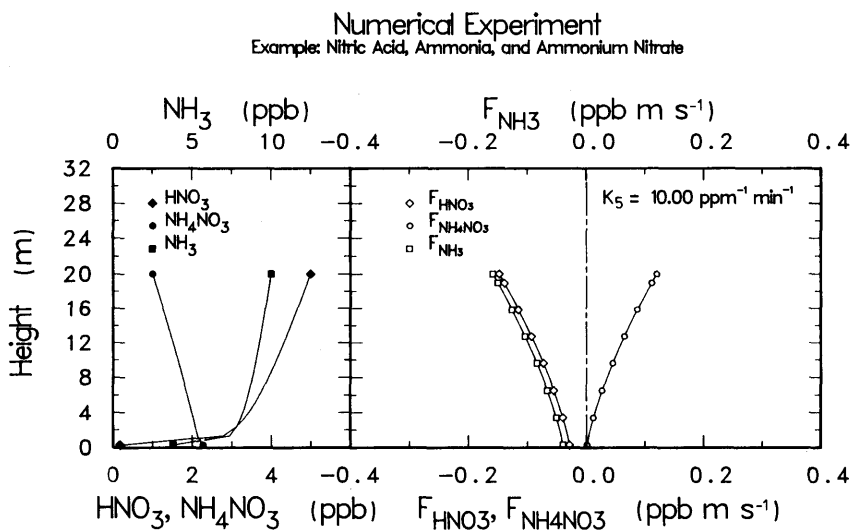
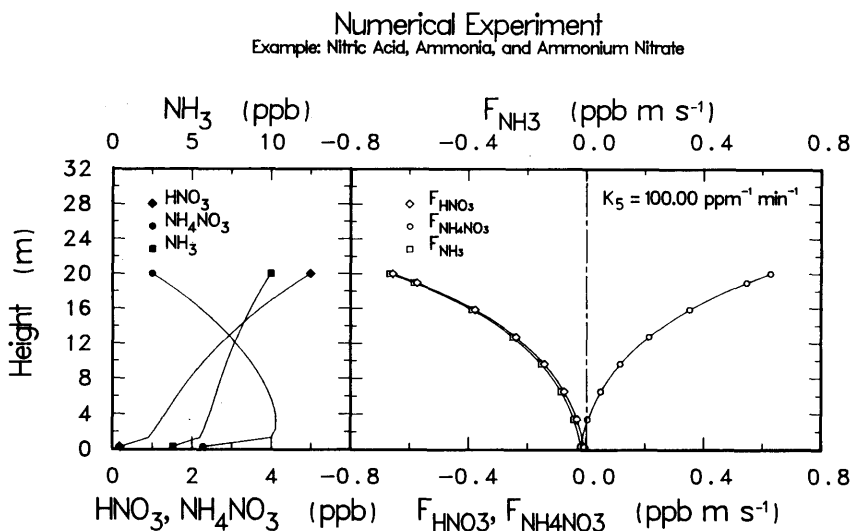


Fig. 3. Vertical profiles of concentrations and turbulent fluxes of HNO₃, NH₃, and NH₄NO₃ for different values of the reaction rate constant k_5 (with reference to Kramm, 1992).

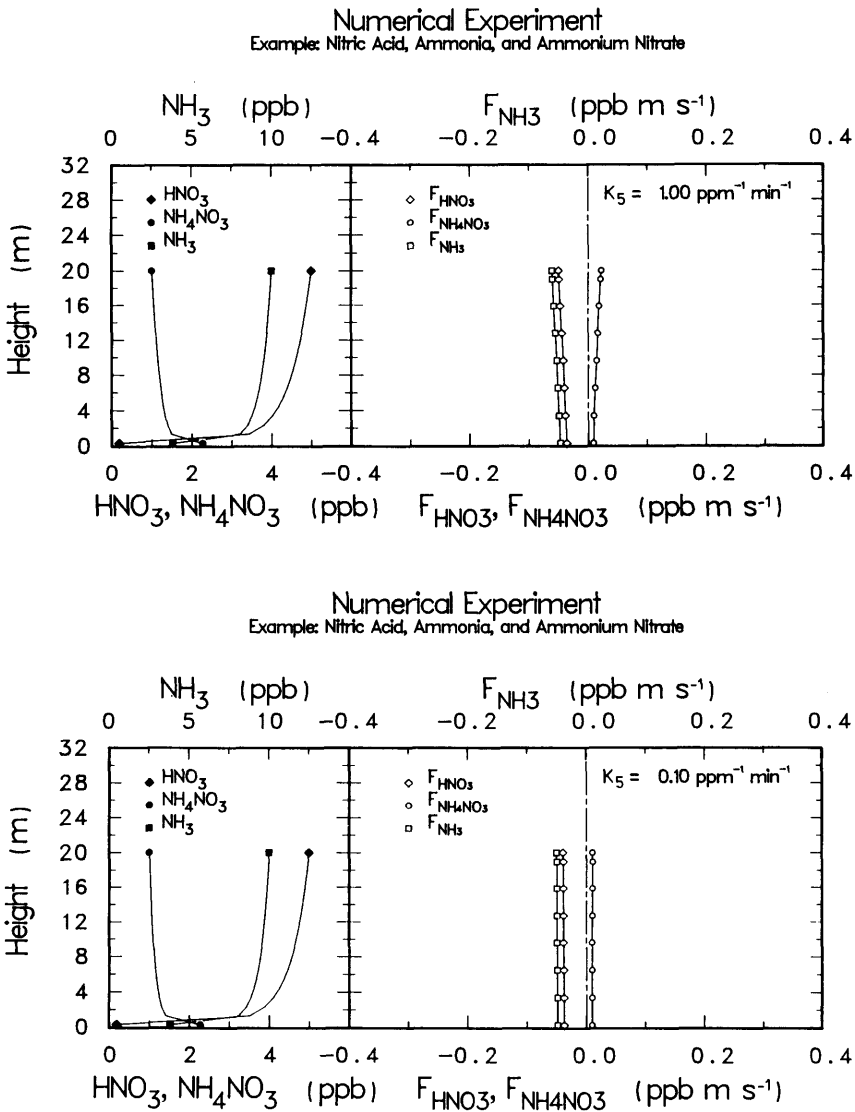


Fig. 4. Vertical profiles of concentrations and turbulent fluxes of HNO_3 , NH_3 , and NH_4NO_3 for different values of the reaction rate constant k_5 (with reference to Kramm, 1992).

the fluxes of HNO_3 , NH_3 , and NH_4NO_3 are nearly height-invariant. For higher values of k_5 (which lead to shorter response times) the flux divergences of these trace species increase, and, hence, the related turbulent fluxes become more and more dependent on height (see Kramm, 1992). Note, that the chemical response times calculated for these cases are ranging from 10^2 s for $k_5 = 100$

$\text{ppm}^{-1} \text{min}^{-1}$ to 10^5 s for $k_5 = 0.1 \text{ ppm}^{-1} \text{min}^{-1}$ (see Kramm, 1992). Data of Larson and Taylor (1983) are indicating a chemical response time of about 100 s and those of Richardson and Hightower (1987), several hundred minutes. With regard to these uncertainties we are considering the constant flux approach only as a first approximation (at best), when NH_3 is present.

This work reports studies on the dry deposition of gaseous nitric acid based on some independent HNO₃ measurements made during two joint field experiments which investigated exchange of NO, NO₂ and O₃ over (a) low vegetation (grassland, LOVENOX, Halvergate, UK, September 1989) and over (b) a wheat canopy (ecosystem wheat, Manndorf, Germany, July 1990). The HNO₃ concentration measurements at Halvergate were performed by AEA Harwell using tubular denuder techniques (see Dollard et al., 1990), those at Manndorf were made by Istituto sull'Inquinamento Atmosferico applying annular denuders (see Perrino et al., 1990; Possanzini et al., 1992).

Dry deposition analysis was performed on the basis of the constant flux approach and assuming that HNO₃ is transported by turbulence similarly to sensible heat and water vapour (see, e.g., Businger, 1986). The relevant micrometeorological fluxes were determined by two independent methods, i.e., by the energy balance method (requiring measurements of net radiation, soil heat flux and Bowen ratio) and by the aerodynamic profile method (relying on wind and temperature measurements at several heights). The data have also been used to check sublayer Stanton numbers, B_c , which are of basic importance in determining the viscous sublayer resistance yet not well quantified.

2. Theoretical background

Bowen ratio and aerodynamic profile techniques are appropriate methods to study the transport of (quasi-)conservative trace constituents within the atmospheric surface layer. Within this frame, it is assumed that the vertical transport of a trace gas entity towards or from the Earth's surface may be written as (see, e.g., Businger, 1973; Biscoe et al., 1975):

$$F_c = -K_c \frac{\partial c}{\partial z}, \quad (5)$$

where F_c is the flux of species c , K_c is the eddy diffusivity, $\partial c/\partial z$ is the vertical gradient of the (volumetric) concentration, and z is the height above ground.

For (quasi-)constant flux conditions which imply that the species measured is chemically

conservative, eq. (5) may be integrated to relate the flux F_c to a finite difference Δc . Expressing the meteorological fluxes of sensible heat, H , and latent heat, E , as relations analogous to eq. (5) with K_h and K_e being the respective eddy diffusivities, and assuming $K_c = K_e = K_h$, the integrated relations for the various fluxes may be written as (see, e.g., Herbert and Kramm, 1981):

$$\begin{Bmatrix} F_c \\ H \\ E \end{Bmatrix} = -\frac{1}{r_t} \begin{Bmatrix} \Delta c \\ (\rho c_p) \Delta \theta \\ (\varepsilon \lambda \rho / p) \Delta e \end{Bmatrix} = \text{const.}, \quad (6)$$

with

$$r_t = \int_{z_1}^{z_2} K_h^{-1} dz, \quad (7)$$

where Δ denotes the difference of concentration, c , potential temperature, θ , and water vapour pressure, e , respectively, across the height interval $\Delta z = z_2 - z_1$ ($z_2 > z_1$). Here, ρ is the density of air, c_p is the specific heat of dry air at constant pressure, ε is the ratio of molecular weight of water vapour to that of dry air ($\varepsilon \approx 0.622$), λ is the latent heat of vaporization of water, and p is the atmospheric pressure.

Relations (6) are written in a form analogous to Ohm's law (flux = potential difference/resistance); thus, the integral expression r_t (eq. (7)) is readily identified as a *bulk* (turbulent) resistance of the air against mass transfer with respect to the height interval $\Delta z = z_2 - z_1$ (see Fowler, 1978 and 1984; Herbert and Kramm, 1981). The reciprocal of r_t has dimensions of a velocity and may be regarded as a transfer velocity, v_{tr} , given by:

$$v_{tr} = r_t^{-1} = -(\rho c_p)^{-1} \frac{H}{\Delta \theta} = -\left(\frac{p}{\varepsilon \lambda \rho}\right) \frac{E}{\Delta e}. \quad (8)$$

Dry deposition is often described in terms of a deposition velocity, v_d , defined by (see Chamberlain, 1961)

$$v_d(z) = -\frac{F_c}{c(z)}, \quad (9)$$

and so

$$v_d(z) = \frac{\Delta c}{c(z)} v_{tr}. \quad (10)$$

Determination of v_d for a trace gas species from eq. (10) requires measurements of the concentrations of the trace gas at two levels (z_1, z_2) and knowledge of the meteorological transfer term v_{tr} ($=r_t^{-1}$). Two independent methods are used to provide the relevant meteorological quantities.

2.1. Aerodynamic profile method

Integration of eq. (7) in the frame of the constant flux approach yields (see Kramm, 1989a):

$$r_t = \frac{1}{u_* \kappa} \left(\ln \frac{z_2 - d}{z_1 - d} - \Psi_h \left(\frac{z_2 - d}{L}, \frac{z_1 - d}{L} \right) \right), \quad (11)$$

where the friction velocity, $u_* = (\tau/\rho)^{1/2}$ (τ = flux of momentum or shear stress), is defined by its integral relation

$$u_* = \frac{\kappa \Delta u}{\ln \frac{z_2 - d}{z_1 - d} - \Psi_m \left(\frac{z_2 - d}{L}, \frac{z_1 - d}{L} \right)}, \quad (12)$$

and where κ is von Kármán's constant ($\kappa = 0.4$), $\Delta u = u_2 - u_1$ is the difference of wind speed u across $\Delta z = z_2 - z_1$, d is the zero plane displacement, L is the Monin-Obukhov stability length, and Ψ_h and Ψ_m are the dimensionless integral stability functions for heat and momentum, respectively (see Paulson, 1970; Kramm, 1989a).

Eqs. (11) and (12) together with relations (6) provide the basis for the so-called *aerodynamic profile* method where the meteorological quantities ($H, \Delta\theta$), ($E, \Delta e$) and ($u_*, \Delta u$) as well as L, d and z_0 (z_0 = roughness length) are determined from vertical profiles of temperature, humidity and wind speed (see Kramm, 1989b). The method is error prone for very stable stratification (with low wind speed and temperature inversion) or in the brief transition phase between lapse and inversion conditions, when steady-state conditions are not expected (see Kramm, 1989b).

2.2. Energy balance (Bowen ratio) method

Eqs. (6), of course, express the concept of Bowen ratio similarity, and one immediately derives the basic relations of the so-called *modified Bowen ratio method* (see Biscoe et al., 1975; Businger, 1986):

$$F_c = (\rho c_p)^{-1} H \frac{\Delta c}{\Delta \theta} = \left(\frac{p}{\varepsilon \lambda \rho} \right) E \frac{\Delta c}{\Delta e}. \quad (13)$$

A simple but viable method to obtain H and E is based on the energy budget at the ground where the net radiation, R_n , is partitioned between the turbulent heat fluxes, $H + E$, and the soil heat flux, G , according to

$$R_n = H + E + G. \quad (14)$$

Introducing the Bowen ratio $\beta = H/E$ via eqs. (6), i.e.,

$$\beta = \left(\frac{c_p p}{\varepsilon \lambda} \right) \frac{\Delta \theta}{\Delta e}, \quad (15)$$

and rearranging eq. (14) gives:

$$H = \frac{R_n - G}{1 + \beta^{-1}}, \quad (16a)$$

$$E = \frac{R_n - G}{1 + \beta}. \quad (16b)$$

Some measurements of the energy balance terms R_n and G and the Bowen ratio β are, therefore, necessary to provide the meteorological parameters ($H, \Delta\theta$) and ($E, \Delta e$) required in eqs. (8) and (6). No stability corrections have to be applied with the energy balance (Bowen ratio) approach. The method fails, however, when the Bowen ratio approaches -1 . This typically occurs twice per day during brief transition periods in the morning and in the afternoon. The method is also error prone during nighttime or in other low flux situations when inaccuracies in measurements of R_n and G are comparable to the micrometeorological fluxes (see, e.g., Whiteman et al., 1989).

2.3. Resistance analogy

Dry deposition is often discussed in terms of a flux-resistance analogy which includes turbulent (r_t), molecular-turbulent (r_{mt}) and surface (r_s) resistances. The molecular-turbulent resistance can be introduced by:

$$F_c = - \frac{c_1 - c_s}{r_{mt}} = - \frac{c_2 - c_s}{r_t + r_{mt}}, \quad (17)$$

with c_2, c_1 , and c_s denoting the concentrations at heights z_2, z_1 , and at the foliage surface. Next, the flux F_c at the interface *atmosphere-biosphere* can be parameterized for low horizontally uniform

vegetation by (see Kramm et al., 1991; Kramm et al., 1993; and Appendix A)

$$F_c = -\frac{c_s}{r_s}, \tag{18}$$

where the (overall) surface resistance, r_s , is given by the relation

$$\frac{1}{r_s} = \frac{1}{r_{st} + H^*r_{int}} + \frac{1}{r_{cu}} + \frac{1}{H^*r_{w,f}} + \frac{1}{r_{mt,g} + r_{sl,tot}}. \tag{19}$$

Here, r_{st} is the stomata resistance, r_{int} is the internal resistance (see O'Dell et al., 1977), r_{cu} is the cuticular resistance, $r_{w,f}$ is the resistance of leaf wetness, $r_{mt,g}$ is the molecular-turbulent resistance for the exchange between the foliage and the ground, $r_{sl,tot}$ is the total resistance of the soil, and H^* is Henry's law constant for HNO₃. Note, that r_{st} , r_{int} , r_{cu} , $r_{w,f}$, and $r_{sl,tot}$ are scaled by the wetness factors $\sigma_{w,f}$ and $\sigma_{w,sl}$ ($0 \leq \sigma_w \leq 1$ for both cases) which represent fractional foliage surface and fractional ground surface covered by water. Furthermore, r_{st} , r_{int} , r_{cu} , and $r_{w,f}$ are scaled by the leaf area index (for details see Appendix A). Eqs. (17) and (18) yield

$$F_c = -\frac{c_2}{r_t + r_{mt} + r_s}, \tag{20}$$

and, considering relation (9),

$$v_d(z_2) = \frac{1}{r_t + r_{mt} + r_s}. \tag{21}$$

Since H^* is very small (of the order of 10^{-7} , see Schwartz, 1986), H^*r_{int} and $H^*r_{w,f}$, as well as $H^*r_{w,sl}$ (a part of $r_{sl,tot}$, see Appendix A) are much smaller than r_{st} and $r_{mt,g}$. Therefore, the surface resistance can be approximated by:

$$r_s = \begin{cases} \left(\frac{1}{r_{st}} + \frac{1}{r_{cu}} + \frac{1}{r_{sl} + r_{mt,g}} \right)^{-1}, & \text{for } \sigma_{w,f} = \sigma_{w,sl} = 0 \\ H^*r_{w,f}, & \text{for } \sigma_{w,f} = \sigma_{w,sl} = 1. \end{cases} \tag{22}$$

Since there is no evidence that in the case of HNO₃ the resistance $r_{sl} + r_{mt,g}$ is much smaller than r_{st}

and/or r_{cu} , it is to be expected that in the case of dry surfaces the leaf resistances cannot be ignored. Note, that values of the total leaf conductance (inverse of the total leaf resistance) of HNO₃ to leaf surfaces for daytime conditions, which are presented on one-sided and total leaf area basis, respectively, were summarized for different tree species by Hanson and Lindberg (1991). These values refer to total leaf resistances which are ranging from 83 s/m (*Ulmus americana*) to $2.5 \cdot 10^3$ s/m (*Pinus strobus*).

Because in the case of surface wetness the effective water resistance $H^*r_{w,f} \ll r_t + r_{mt}$, eq. (20) reduces to $F_c = -c_2 / (r_t + r_{mt})$ or (see also Fowler, 1984)

$$v_d(z_2) = \frac{1}{r_t + r_{mt}}. \tag{23}$$

Thus, in the wet case, the surface is behaving as a perfect sink and all molecules arriving at the surface are being absorbed. Since the effective water resistances, $H^*r_{w,f}$ and $H^*r_{w,sl}$, are much smaller than the canopy resistance for dry surfaces, we conclude that even for small wetness factors $\sigma_{w,f}$ and $\sigma_{w,sl}$, the canopy resistance can be ignored. Experimental work over different types of low vegetation (see Huebert and Robert, 1985; Harrison et al., 1989) gives some evidence of rather small surface resistances r_s of HNO₃ which might be explained by the high solubility of HNO₃ in aqueous solution (see also Wesely, 1989).

2.4. Determination of sublayer Stanton number B_c

Following Owen and Thomson (1963), the molecular-turbulent resistance, r_{mt} , related to the quasi-neutral sublayer from $z = z_1$ to $z = 0$ (the foliage or the ground surface) may be expressed by (see Kramm et al., 1992, and Appendix B):

$$r_{mt} = \frac{u_1}{u_*^2} + \frac{Sc}{u_*} \int_0^{Re_* \cdot r} \frac{dRe_*}{1 + Sc K_m / v} = \frac{u_1}{u_*^2} + (u_* B_c)^{-1}, \tag{24}$$

$I(Sc, Re_*, r)$

where $(u_* B_c)^{-1}$ is introduced to account for the diffusional transport across the viscous layer close to the surface and $B_c = (Sc I(Sc, Re_*, r))^{-1}$ is the sublayer Stanton number. The term $(u_* B_c)^{-1}$ is known to be strongly influenced by molecular diffusivity of the material being transferred (see

Hicks et al., 1987). In case of vegetation and fibrous roughness elements $B_c^{-1}(\text{HNO}_3) = 7.25$ is proposed by Hicks et al. (1987) to give

$$(u_* B_c)^{-1} = 7.25 u_*^{-1}. \quad (25)$$

An opportunity to derive B_c (and so to check $B_c^{-1} = 7.25$) is offered when eq. (23) is adopted as being valid for HNO_3 vapour. Then eqs. (23) and (24) may be combined to give:

$$B_c^{-1} = u_* \left(\frac{1}{v_{d,2}} - \left(r_1 + \frac{u_1}{u_*^2} \right) \right), \quad (26)$$

which is denoted as the residuum method. Note, that determination of $v_{d,2} = v_d(z_2)$ (via eq. (10)) requires HNO_3 concentration measurements. Further, $r_1 + u_1/u_*^2$ ($= u_2/u_*^2$ for neutral and stable conditions, $L \geq 0$) is sometimes denoted in the literature as the aerodynamic resistance r_a (see, e.g., Hicks et al., 1987).

Another approach to obtain B_c is based on the heat transfer relationship for rough surfaces derived by Owen and Thomson (1963) (see also Galbally, 1971; Kramm, 1989a), i.e.,

$$B_h^{-1} = \gamma \text{Re}_{*,r}^m \text{Pr}^n, \quad (27)$$

and, therefore,

$$B_c^{-1} = B_h^{-1} \left(\frac{\text{Sc}}{\text{Pr}} \right)^n, \quad (28)$$

where B_h is the sublayer Stanton number for heat, Pr is the Prandtl number for air ($= 0.71$), $\text{Re}_{*,r} = u_* z_r / \nu$ is the roughness Reynolds number, z_r is the sublayer thickness, ν is the kinematic viscosity of air ($\approx 0.15 \cdot 10^{-4} \text{ m}^2 \text{ s}^{-1}$), $\text{Sc} = \nu / D_c$ is the Schmidt number (≈ 1.08), D_c is the molecular diffusivity of HNO_3 in air ($\approx 0.14 \cdot 10^{-4} \text{ m}^2 \text{ s}^{-1}$), and γ , m , and n are empirical quantities.

Adopting $\gamma = 0.52$, $m = 0.45$, and $n = 0.80$ (see Owen and Thomson, 1963) it follows from eqs. (27) and (28):

$$B_c^{-1} \approx 83 z_r^{0.45} u_*^{0.45}, \quad (29)$$

with z_r in m and u_* in m s^{-1} . In this contribution, it is suggested that $z_r = d + z_0$ which is a characteristic height of any canopy layer.

Ignoring d for a moment and assuming $z_r = z_0 = 0.01 \text{ m}$ (representative for many grassland field

sites), eq. (29) reduces to $B_c^{-1} = 10.45 u_*^{0.45}$ (giving $B_c^{-1} = 6.9$ for $u_* = 0.4 \text{ m s}^{-1}$). This formula is also in broad agreement with $B_c^{-1} = 10.2 u_*^{1/3}$ (see Businger, 1986) used by Harrison et al. (1989). Using $z_r = 0.01 \text{ m}$ as a reference eq. (29) shows that B_c^{-1} increases by the factor $f_d = (100 z_r)^{0.45}$ for larger z_r . In case of the Manddorf wheat field site z_r was about 0.70 m giving $f_d \approx 7$.

It should be mentioned that the values of γ , m , and n proposed by Owen and Thomson are best fit parameters for heat transfer over different small roughness elements and are only valid for $z_r = 30 z_0$. Other wind tunnel and field experiments suggested slightly different values of the exponents m and n but rather large deviations for γ (see Brutsaert, 1982; Businger, 1986) which may be caused by different $z_r - z_0$ relations. Since B_c^{-1} depends also on z_r (see eq. 24), it is expected that for tall fibrous canopy elements γ , m , and n may be quite different.

3. Results and discussion

3.1. Halvergate Marshes, Norfolk, September 1989

At Halvergate near Great Yarmouth, Norfolk, HNO_3 concentration was measured by AEA Harwell at heights of 0.25 m , 0.75 m , 1.45 m , and 2.00 m using sodium fluoride coated denuder tubes (see Dollard et al. 1990). This site is a large expanse of drained marshland (grass, grazed pasture), 1 m above sea level. Fetch extended to over 1 km in most directions and provided excellent micrometeorological conditions, but the disposition of the field equipments restricted the usable fetch to the westerly sector. The site receives only small fertiliser input. However, cattle were removed from the site 2 weeks before the field experiment was performed (see Hargreaves et al., 1992).

Prior to use the denuder tubes (glass tubes) were soaked in chromic acid overnight and rinsed thoroughly with deionised water. Each tube was 95 cm in length and of id 3 mm , the uncoated prelaminal flow region was defined by an etch mark 15 cm from the inlet. The remaining 80 cm was coated with the NaF absorbent. The coating solution was made up in ethanol (spectrosol grade) and was applied to the tubes after all traces of rinsing water had been removed with pure ethanol. Once coated the tubes were dried in a

light stream of air from a cylinder. During all these procedures gloves were worn to minimize contamination. The tubes were usually made up immediately prior to their use in profile determinations.

Flow through each tube was controlled by critical orifices to 3 l/min. The exposure time varied for each run and was decided upon on the basis of a judgement on the likely ambient concentrations of HNO₃ (for analytical requirements) as well as uncertainties introduced into flux measurements made over long periods (2–3 h).

Following exposure the tubes were carefully removed and rinsed using 5 ml of quartz distilled water. The solutions were stored at 4°C in washed sample pots until they were analysed. All the denuder extracts were analysed for NO₃ on a Dionex ion chromatograph.

We present here some results from the main comparative observing periods on 19, 20 September 1989, with preference to a more detailed description of the micrometeorological environment, the transport processes, and the aerodynamic profile method (using data from IFU, ITE and AEA).

On September 19th two HNO₃ daytime (3 h) runs were performed. The ambient meteorological situation is indicated from Figs. 5 and 6 which show the daytime variation of net radiation R_n , sensible heat H , and friction velocity u_* (20 min means). The normal pattern of a fine weather day becomes evident with R_n peaking at about 400 W m⁻² at midday. Sensible heat fluxes reached maximum values of only about 150 W m⁻² (due to a relatively large evaporation rate from the grass indicated by Bowen ratios of 0.7 to 0.9). Friction velocity u_* reached approximately 0.40 m s⁻¹ with moderate winds of 3 to 4 m s⁻¹ at $z = 0.50$ m.

Different measuring systems and methods were utilized to obtain these results (see legends of Figs. 5, 6). All things considered, the agreement between the different methods was quite satisfactory and gives confidence in the measurements.

Fig. 6c shows the transfer velocity v_{tr} with respect to the height interval $z_1 = 0.50$ m and $z_2 = 2.45$ m (lower and upper level of the ITE Bowen ratio system) as evaluated by the energy balance method (ITE) and the aerodynamic

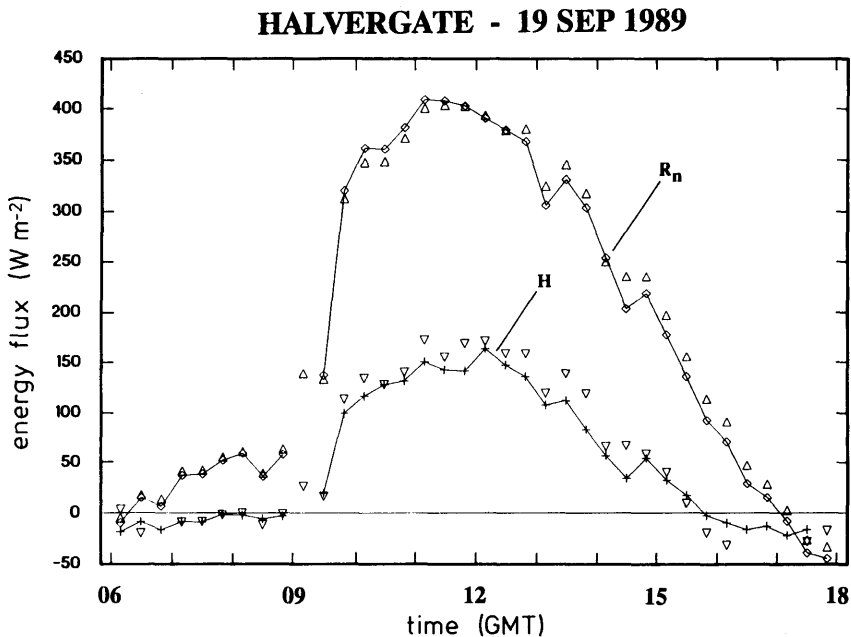


Fig. 5. Daytime variation of net radiation R_n and sensible heat flux H (20 min means) over short grass ($h \approx 0.1$ m) at Halvergate on 19 September 1989. R_n measurements were performed with a Schulze-Lange type radiometer (\diamond and solid line, IFU) and with a Campbell Q4 net radiometer (\triangle , ITE). H values are derived by the profile method (+ and solid line, IFU) and by the energy balance method (∇ , ITE).

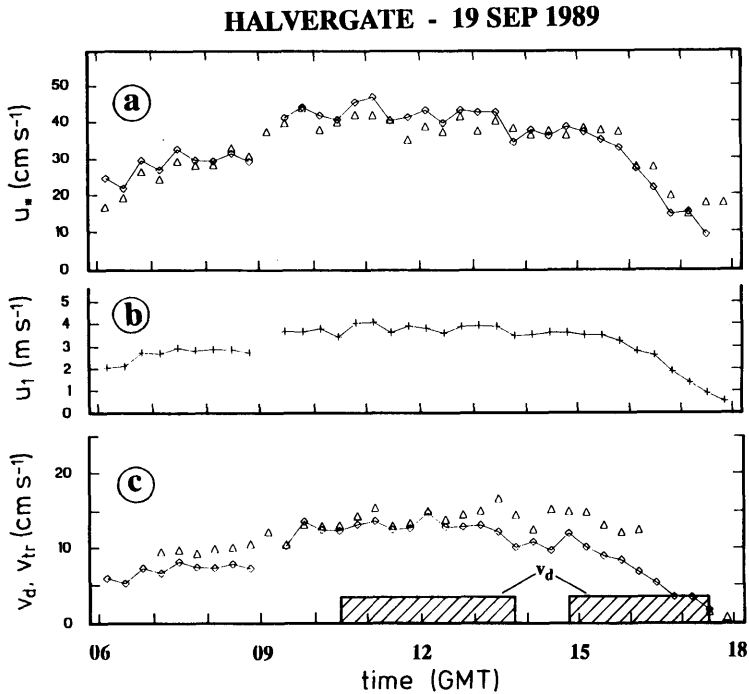


Fig. 6. Daytime variation of (a) friction velocity u_* derived from wind and temperature profile measurements performed by IFU (\diamond and solid line) and AEA (Δ); (b) wind speed u_1 at $z_1 = 0.52$ m (IFU); (c) transfer velocity v_{tr} according to the profile method (\diamond and solid line, eqs. (8, 11), IFU) and to the energy balance method (Δ , eq. (8), ITE). Also shown: dry deposition velocity v_d (at $z = 1.0$ m) for two HNO_3 runs (AEA) according to eq. (10). Halvergate, 19 September 1989.

profile method (IFU). Both methods agree quite well during most of the time with the exception of the afternoon hours where the values obtained by the Bowen ratio method are systematically higher. Non-stationary conditions and uncertainties in the $R_n - G$ measurements at large zenith distances might be reasons for these discrepancies. Moreover, some of these differences may also be caused by real differences across the field since the two

measurement systems were separated by approximately 100 m.

HNO_3 deposition velocities v_d of about 3.5 cm s^{-1} for both measuring periods (see Fig. 6c) were derived according to eq. (10) using the data given in Table 1.

The B_c^{-1} value as evaluated according to eq. (26) (*residuum method*) is much smaller than $B_c^{-1} = 7.25$ for the first run and even negative

Table 1. Data analysis for HNO_3 dry deposition over grassland at Halvergate on 19 September 1989 (indices 1, 2 refer to heights $z_1 = 0.50$ m and $z_2 = 2.45$ m)

Period (GMT)	u_* (m s^{-1})	u_1 (m s^{-1})	v_d ($z = 1$ m) (m s^{-1})	c ($z = 1$ m) ($\mu\text{g m}^{-3}$)	Δc ($\mu\text{g m}^{-3}$)	v_{tr} ($=r_1^{-1}$) (m s^{-1})	$v_{d,2}^{-1}$ (s m^{-1})	r_{mt} (s m^{-1})	(*) B_c^{-1}	(**) B_c^{-1}	(***) B_c^{-1}	(****) L (m)
10:35–14:00	0.42	3.83	0.035	0.58	0.16	0.127 ⁽⁺⁾	33	39	1.4	14.6	–50.0	
14:41–17:41	0.26	2.58	0.034	0.47	0.24	0.066	38	66	(–3.9)	11.8	(28.6)	

(*) Eqs. (24, 25); (**) eq. (26); (***) eq. (29) with $z_r = d + z_o = 0.05$ m.

(⁺) For comparison: $v_{tr} = 0.145$ m/s (energy balance method, ITE).

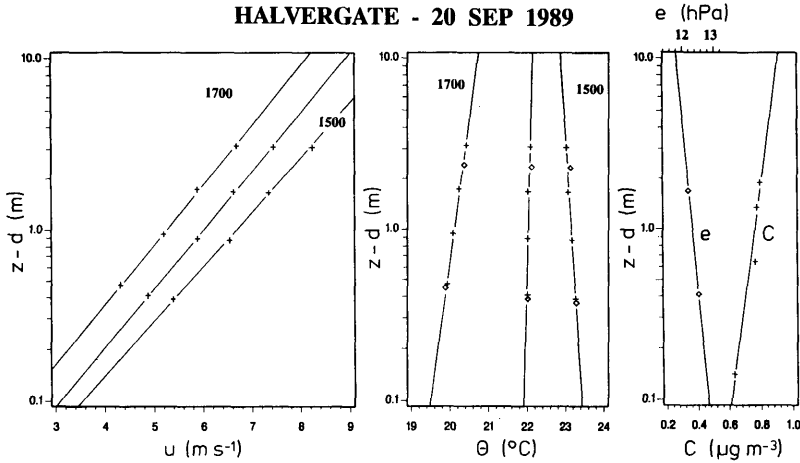


Fig. 7. Mean profiles of wind speed u , potential temperature θ , water vapour pressure e and HNO₃ concentration c for the measuring period 14:34–17:30 GMT at Halvergate on 20 September 1989. ITE temperature measurements are indicated by (\diamond). HNO₃ measurements were performed by AEA. Additional 20 min mean u and θ profiles are provided for 15:00 GMT and 17:00 GMT.

(which is physically impossible, see eq. (24)) for the 2nd run. We attribute this discrepancy mainly to errors in the determination of the HNO₃ concentration fraction $\Delta c/c$ (with a mean precision of the applied denuder technique being about 16% under field conditions, see Dollard et al., 1990). A diminution in $v_d(z_2)$ ($\sim \Delta c/c$) of 30%, for example, would shift the residual $B_c^{-1} = 1.4$ to $B_c^{-1} = 7.6$ (other terms unchanged). Values of B_c^{-1} obtained from eq. (29) are about twice as large as $B_c^{-1} = 7.25$ (according to $f_d \approx 2$).

The other Halvergate HNO₃ run to be discussed here was performed under high wind speed (5 to 7 m s⁻¹ at $z = 1.0$ m) and near neutral (well mixed) conditions on 20 September.

Fig. 7 shows the mean profiles of wind speed (u), potential temperature (θ), water vapour pressure

(e) and HNO₃ concentration (c) over the measuring period 14:34 to 17:30 GMT. Additional u - and θ -profiles (20 min means for 15:00 and 17:00 GMT) are included to evidence the 3-h measuring interval as steady cooling period associated with decreasing wind speed but only minor changes of the near neutral state (ascertained by a close agreement between IFU and ITE temperature profiles at different stages).

The HNO₃ concentration profile, which appears to be quite logarithmic, was used to derive a deposition velocity v_d of 1.7 cm s⁻¹ according to eq. (10). For details of data analysis see Table 2. The transfer velocity v_{tr} ($=r_t^{-1}$) was calculated with IFU profile data ($E = 85$ W m⁻², $\Delta e = -0.33$ hPa, $u_* = 0.50$ m s⁻¹, $d = 0.11$ m) according to eqs. (8) and (11) to yield $v_{tr} = 14.1$ cm s⁻¹.

Table 2. Data analysis for HNO₃ dry deposition over grassland at Halvergate on 20 September 1989, 14:34–17:30 GMT; (indices 1, 2 refer to heights $z_1 = 0.52$ m and $z_2 = 1.79$ m)

$u_*^{(+)}$ (m s ⁻¹)	u_1 (m s ⁻¹)	$v_d(z = 1 \text{ m})$ (m s ⁻¹)	$c(z = 1 \text{ m})$ ($\mu\text{g m}^{-3}$)	Δc ($\mu\text{g m}^{-3}$)	$v_{tr}(=r_t^{-1})$ (m s ⁻¹)	$v_{d,2}^{-1}$ (s m ⁻¹)	r_{mt} (s m ⁻¹)	(*) B_c^{-1}	(**) B_c^{-1}	(***) L (m)
0.50	4.90	0.017	0.75	0.09	0.141	62	34	17.9	23.2	∞

(*) Eqs. (24, 25); (**) eq. (26); (***) eq. (29).

Further measured and derived quantities: $d = 0.11$ m⁽⁺⁾, $z_o = 0.009$ m⁽⁺⁾, $E = 85$ W/m², $\Delta e = -0.33$ hPa (IFU), $E \approx R_n - G = 105$ W/m² (energy balance, ITE).

(+) For comparison: $u_* = 0.52$ m/s, $d = 0.10$ m, $z_o = 0.007$ m (AEA).

Unfortunately, no useful water vapour pressure data are available from the Bowen ratio system for this period. With $\beta \approx 0$ (neutral conditions), however, a latent heat flux $E \approx 105 \text{ W m}^{-2}$ can be estimated via eq. (16b) (i.e., $E \approx R_n - G$) which compares well with the IFU profile data.

Values of B_c^{-1} of 17.9 according to eq. (26) and 23.2 according to eq. (29) show a high degree of coincidence between both methods, which, however, should not be overrated for reasons mentioned earlier.

3.2. Manndorf wheat field site, Lower Bavaria, July 1990

HNO_3 measurements at Manndorf near Plattling/Lower Bavaria, 300 m above sea level (Danube River valley, approximately 40 km northwest of Passau) were performed by the Istituto sull'Inquinamento Atmosferico using annular denuder techniques with a relative precision of better than 5%. This site was a large homogeneous wheat (*Triticum aestivum* L.) field (a mature wheat canopy 0.90 to 1.10 m tall with a leaf

area index of about $\text{LAI} \approx 7$, B. Huber, private communication) which had a length of 700 m (E-W direction) and a width of 220 m (N-S direction). The differences in levels were not more than 1.5 m across the field as a whole. The field equipments were disposed along the N-S direction. They restricted the usable fetch to the westerly sector (approximately 400 m) and the easterly sector (approximately 300 m; see Meixner and Schröder, 1991).

The annular denuder equipment consisted of two thermostated sampling units, each accommodating 7 annular denuder-filter pack lines (see Perrino et al., 1990; Possanzini et al., 1992). These units were operated by microprocessor controlled electronic samplers. The sampling train consisted of two NaCl-coated denuders, a Na_2CO_3 /glycerol coated denuder, a citric acid-coated denuder, a Teflon cyclone ($2.5 \mu\text{m}$ cut size), a Teflon filter, a Nylon filter, and a citric acid coated filter in sequence. The 1st 2 denuders served to measure HNO_3 , the 3rd denuder removed SO_2 , and the 4th denuder absorbed NH_3 . Fine particles were

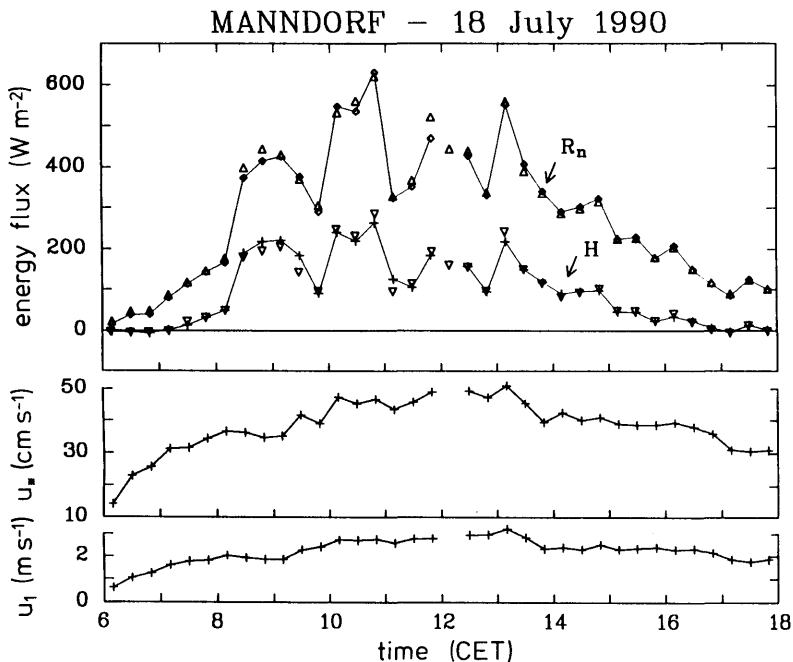


Fig. 8. Daytime variation of net radiation R_n and sensible heat flux H (20 min means) at Manndorf on 18 July 1990. R_n measurements by Schulze-Lange type radiometer (\diamond , and solid line) and by Campbell Q5 (Δ) net radiometer. H values by the profile method (+ and solid line) and by the energy balance method (∇). Also shown: friction velocity u_* (profile method) and wind speed u_1 at $z_1 = 1.30 \text{ m}$.

collected on the front Teflon filter, whereas the subsequent filters served to trap HNO_3 and NH_3 arising from the dissociation of NH_4NO_3 (see reaction R6) volatilized from the first filter. Note, that the concentration data of NH_3 and NH_4NO_3 measured at Mandorf were of the same order as shown in Figs. 3 and 4. But the uncertainties in reaction structure and reaction rate constants mentioned earlier prevent any improvement of flux calculations on the basis of the nitrous triad $\text{HNO}_3\text{-NH}_3\text{-NH}_4\text{NO}_3$.

The two thermostated sampling units were installed at $z_1 = 1.30$ m (approximately 0.30 m above vegetation), and at $z_2 = 3.83$ m. Consecutive sampling periods of 1 h were chosen to better adjust to meteorological variability. Samples were collected at an air flow rate of 12 l/min between 12–19 July. The relevant micrometeorological data (20 min means) were provided by the IFU profile mast equipment and by the IFU Bowen ratio system (Campbell Scientific Ltd.).

The data analysis is restricted to the measurements on 13–19 July with dominant westerly (13–14, 17–19 July) and easterly winds. Deposition

flux estimations are based on 1 h means which were derived from the 20 min means of the relevant micrometeorological data.

Figs. 8 to 10 show results from 18 July. The sky was partly cloudy on this day which caused some variability in the thermal pattern during noon hours and prevented a stronger heating of the canopy environment. These conditions are mirrored in Fig. 8 where the daytime evolution of net radiation (R_n) and sensible heat flux (H) together with friction velocity (u_*) and wind speed (u_1) are shown (note the close agreement between different experimental approaches for the R_n - and H -pattern).

Fig. 9 shows a comparison between sensible heat fluxes derived by the aerodynamic profile method and by the energy balance (Bowen ratio) method. The good agreement suggests that the neglect of any (biomass-) heat storage terms in the energy balance was a reasonable approach under these conditions.

The evolution of HNO_3 concentration c at $z = 2.0$ m (≈ 1 m above vegetation) was already mentioned in the introduction to evidence a

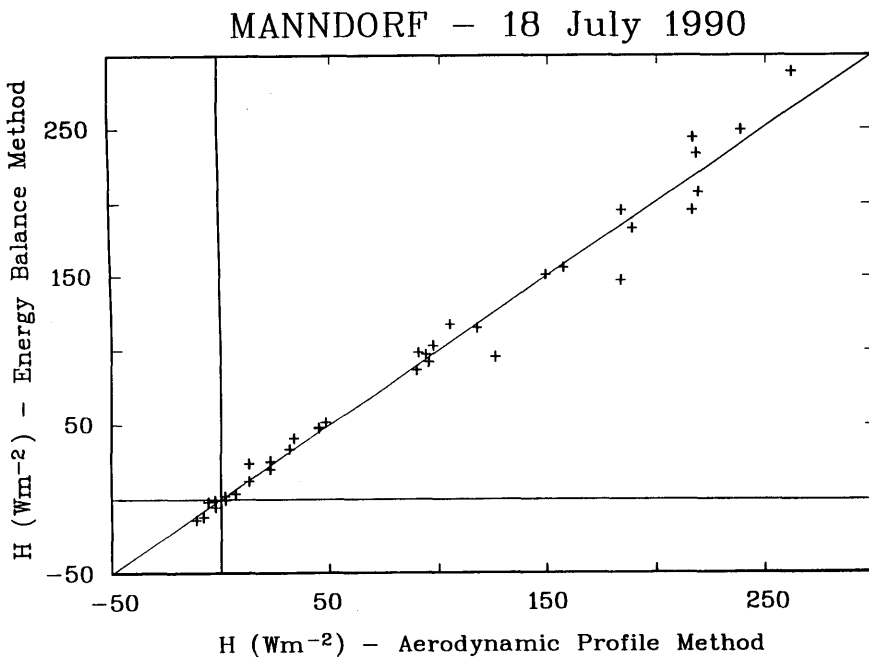


Fig. 9. Comparison of sensible heat fluxes by the profile and the energy balance method (06:20–18:20 CET, $n = 36$, $u_1 > 1.0$ m/s) at Mandorf on 18 July 1990.

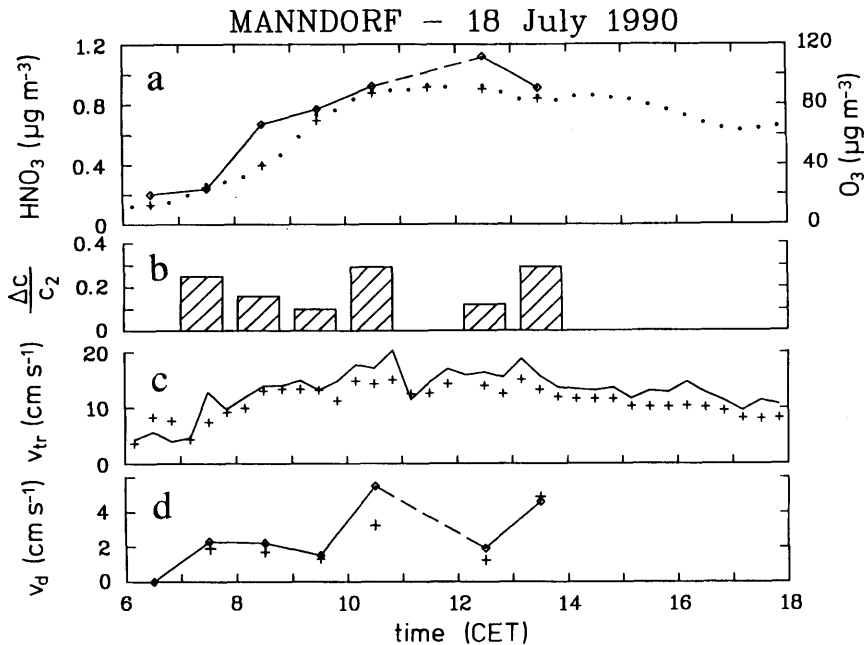


Fig. 10. Time variation of (a) HNO₃ concentration at $z = 2$ m (\diamond : hourly means), O₃ concentration at $z = 4.5$ m ($+$: hourly means, dots: 20 min means); (b) concentration fraction $\Delta c/c$; (c) transfer velocity v_{tr} by the energy balance method (solid line, eq. (8)) and by the profile method ($+$, eqs. (8, 11)); (d) dry deposition velocity v_d at $z = 2$ m according to eq. (10). \diamond : energy balance method, $+$: profile method. Manndorf, 18 July 1990.

photochemically induced increase of HNO₃ before noon. Under these conditions deposition velocities v_d were ranging from 1.3 cm s^{-1} to 4.8 cm s^{-1} (see Fig. 10). Also shown in Fig. 10 is the evolution of concentration fraction $\Delta c/c$ and transfer velocity v_{tr} (determined by different approaches) in order to illustrate the relative importance of $\Delta c/c$ and v_{tr} on v_d in eq. (10). With the turbulent transfer rate v_{tr} remaining nearly constant, the v_d -peak value of about 5 cm s^{-1} is immediately recognized as being caused by changes in the $\Delta c/c$ environment. (Note, that this value is not considered in the subsequent complete data analysis.)

The complete data analysis is summarized in Tables 3, 4. Values of the deposition velocity (also determined for a height at $z = 2.0$ m) are ranging from 0.6 cm/s to 5.0 cm/s with an average value (based on 26 runs) of $2.1 \pm 1.2 \text{ cm/s}$. Values of B_c^{-1} as evaluated by the *residuum method* (eq. 26) cover a wide range from 1.7 to 24.5. Based on the 26 runs with $\Delta c > 0$ (deposition), B_c^{-1} averages to 11.5 ± 7.4 . The B_c^{-1} values obtained from the sub-layer transfer relationship (29) are much larger

and average to $B_c^{-1} = 41.3 \pm 6.5$ (which is about $4 \times$ larger than $B_c^{-1} = 11.5$ and is explained by the sublayer thickness $z_r = d + z_o \approx 0.70 \text{ m}$ resulting in $f_d \approx 7$, see Subsection 2.4).

The data analysis is based on the constant flux approach and the assumptions leading to eqs. (20) to (23). Since no direct measurements of HNO₃ fluxes by eddy correlation techniques were available (fast response HNO₃ sensors do not exist at present), a validation of the modified Bowen ratio and aerodynamic profile methods cannot be performed on the basis of such measurements. Therefore, in order to evaluate our estimations, the flux-resistance relationship postulated by eq. (20) and the associated approach (23) were examined. Note, that the postulated linear relationship between the flux and the mean concentration (see eq. (20)) is only valid when flux divergence effects, in particular caused by chemical processes, are negligible.

Results of this examination are illustrated in Figs. 11 to 15. It may be depicted from Figs. 11 and 12 that linearity between F_c and c according to

Table 3. Data analysis for micrometeorological quantities over mature wheat at Mandorf on July 1990

Day	Period (CET)	z ₀ (cm)	d (cm)	u _* (cm s ⁻¹)	H (W m ⁻²)	L (m)	R _n (W m ⁻²)	DD (deg.)	σ _u * (cm s ⁻¹)	σ _θ * (10 ⁻² K)
13	13-14	12.6	50.9	21.7	115.1	-7.8	633.2	269	1.9	3.8
	14-15	8.0	65.3	20.5	57.5	-13.0	550.4	263	0.5	0.1
14	11-12	11.2	45.3	40.0	285.6	-19.6	680.0	284	0.3	0.7
	12-13	7.7	59.0	38.1	213.4	-22.6	683.7	281	0.3	0.6
	13-14	8.9	50.4	40.5	132.9	-43.6	558.8	296	2.1	3.9
	14-15	9.6	48.3	37.9	93.2	-51.2	534.8	294	0.8	6.0
	15-16	8.1	53.6	34.9	62.6	-59.1	446.4	287	1.7	3.5
15	08-09	7.0	76.7	14.6	20.4	-13.5	230.5	96	0.5	1.5
	09-10	5.9	76.2	17.7	37.0	-13.0	353.2	97	0.1	2.6
	10-11	8.3	63.5	18.1	34.1	-15.1	424.0	107	0.6	2.5
	11-12	8.9	61.1	16.0	92.4	-3.9	508.0	165	<0.1	0.1
16	09-10	7.9	63.3	18.4	118.0	-4.6	494.1	95	1.2	3.3
	10-11	7.1	63.8	17.9	138.7	-3.6	594.0	75	0.7	2.5
	11-12	8.0	71.0	22.1	171.4	-5.5	647.7	303	1.8	1.7
	12-13	7.3	67.8	27.7	102.5	-18.2	551.0	291	1.3	3.0
17	11-12	6.6	63.0	45.4	156.1	-52.2	568.7	312	5.4	1.7
	12-13	8.6	57.8	46.9	24.3	-370.4	245.3	322	4.3	2.8
	14-15	2.4	76.1	39.9	87.1	-63.6	517.3	297	0.1	0.8
	15-16	2.2	76.0	37.7	5.3	-886.3	231.2	296	0.2	2.3
	07-08	7.7	62.1	32.4	15.1	-197.3	111.8	288	2.3	0.8
18	08-09	5.1	72.3	32.6	170.1	-17.9	395.1	285	1.9	2.9
	09-10	6.1	65.4	38.4	151.2	-32.7	364.6	303	4.4	1.4
	10-11	3.6	69.4	39.6	179.6	-30.3	571.2	293	0.1	0.4
	12-13	3.3	69.2	41.2	98.2	-62.5	379.9	296	0.1	0.9
	08-09	6.3	71.8	28.0	41.1	-46.8	150.8	300	2.8	0.9
19	10-11	12.1	44.6	38.5	116.8	-42.8	256.1	293	1.4	1.9

* The "badness of fit" for wind speed, σ_u, and potential temperature, σ_θ, is defined by σ_x = {N⁻¹ ∑_{i=1,N} (x_{m,i} - x_{c,i})²}^{1/2}, where x_{m,i} is the measured value at the height z_i, x_{c,i} is the corresponding calculated value, and N (> 2) is the number of observation levels.

eq. (20) and v_d = v_d(z₂) and u_{*} according to eq. (23) (r_{m1} and r₁ can be considered as functions of u_{*}) exists, but in both cases the scatter is large. Since a linear relationship between v_d and Δc/c₂ exists with a satisfactory accuracy (see Fig. 13), where the micrometeorological quantity v_{tr} = r₁⁻¹ is the proportionality factor (see eq. 10), this large scatter is mainly due to variations in the Δc/c₂ environment (the linearity between F_c and c shown in Fig. 11 might be considered as an indication that the influence of the chemical reactions R5 and R6 is of minor significance). For example: The relative error δv_d/v_d of the deposition velocity can be estimated according to

$$\frac{\delta v_d}{v_d} = \left\{ 2 \left(\left(\frac{\Delta c}{c_2} \right)^{-1} - 1 \right)^2 \left(\frac{\delta c}{c} \right)^2 + \left(\frac{\delta H}{H} \right)^2 + 2 \left(\frac{\delta \theta}{\Delta \theta} \right)^2 \right\}^{1/2}, \tag{30}$$

where δc/c and δH/H are the relative errors with which c and H can be determined, and δθ is the absolute error of the temperature measurements. Expression (30) is derived from eqs. (8) and (10) on the basis of a propagation of errors treatment. Values of δv_d/v_d are listed in Table 4. Taking the typical values δc/c = 3%, δH/H = 25% and δθ = 0.02 K into account, δv_d/v_d is mainly affected

Table 4. Data analysis for HNO_3 dry deposition over mature wheat at Mandorf on July 1990 (index 2 refers to the height $z_2 = 3.83 \text{ m}$)

Day	Period (CET)	c_2 ($\mu\text{g m}^{-3}$)	Δc ($\mu\text{g m}^{-3}$)	F_c ($\mu\text{g m}^{-2} \text{ s}^{-1}$)	$v_d(z=2 \text{ m})$ (cm s^{-1})	$\delta v_d/v_d$ (%)	r_t (s m^{-1})	(*) r_{mt} (s m^{-1})	(**) B_c^{-1}	(***) B_c^{-1}
13	13-14	4.72	0.87	-0.1093	2.55	31.3	8.0	35.2	3.7	39.3
	14-15	4.33	0.92	-0.0788	2.03	29.6	11.7	43.3	4.0	34.7
14	11-12	2.23	0.19	-0.0341	1.60	52.1	5.6	59.9	19.2	46.8
	12-13	2.58	0.67	-0.0974	4.34	27.8	6.9	19.6	2.2	45.8
	13-14	2.09	0.25	-0.0360	1.84	39.9	6.9	51.1	15.4	47.1
	14-15	1.90	0.38	-0.0507	2.99	30.2	7.5	30.0	6.2	45.7
	15-16	2.15	0.33	-0.0379	1.92	34.3	8.7	47.8	11.2	44.0
15	08-09	0.58	0.06	-0.0032	0.58	44.6	18.8	162.6	19.0	29.7
	09-10	0.96	0.08	-0.0052	0.57	53.1	15.3	168.3	24.5	32.4
	10-11	1.30	0.15	-0.0110	0.90	41.1	13.6	104.2	13.9	32.8
	11-12	1.59	0.14	-0.0154	1.01	50.6	9.1	94.4	10.8	31.0
16	09-10	1.12	0.23	-0.0263	2.60	29.9	8.7	33.8	1.7	33.0
	10-11	1.45	0.17	-0.0208	1.52	40.6	8.2	61.4	6.3	32.6
	11-12	1.94	0.16	-0.0187	1.00	53.7	8.5	95.0	16.6	35.8
	12-13	3.06	0.51	-0.0524	1.86	32.8	9.7	48.7	8.4	39.7
17	11-12	1.96	0.19	-0.0268	1.44	46.7	7.1	66.1	24.3	49.6
	12-13	3.71	1.17	-0.1509	4.91	30.9	7.8	16.8	2.6	50.3
	14-15	2.92	0.62	-0.0660	2.53	29.6	9.4	34.8	6.2	46.8
	15-16	2.23	0.53	-0.0466	2.38	63.3	11.4	36.5	5.8	45.6
18	07-08	0.27	0.06	-0.0053	2.23	34.7	11.3	39.5	7.4	42.6
	08-09	0.73	0.11	-0.0127	1.87	34.6	8.7	48.8	10.1	42.7
	09-10	0.81	0.08	-0.0101	1.32	46.0	7.9	72.1	21.9	46.0
	10-11	1.07	0.27	-0.0345	3.68	28.0	7.8	23.3	4.1	46.0
	12-13	1.19	0.13	-0.0153	1.36	42.8	8.5	69.0	23.4	47.4
19	08-09	0.24	0.04	-0.0033	1.48	32.8	12.3	61.4	11.7	39.9
	10-11	1.06	0.31	-0.0446	4.99	27.0	6.9	16.8	17.5	46.0

(*) Eqs. (10, 23); (**) eq. (26); (***) eq. (29) with $z_r = d + z_0$.

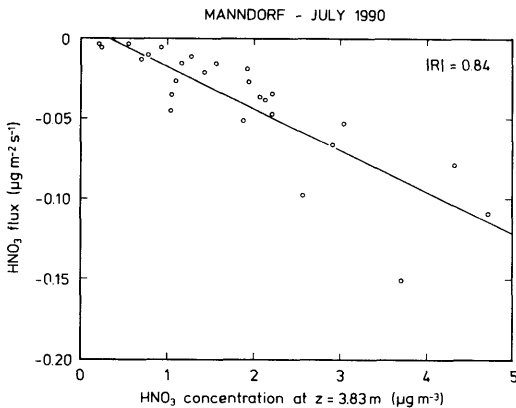


Fig. 11. Relationship between the calculated HNO_3 flux and the HNO_3 concentration measured at $z_2 = 3.83 \text{ m}$ using annular denuder techniques (sampling periods of 1 h), according to eq. (20). R is the correlation coefficient.

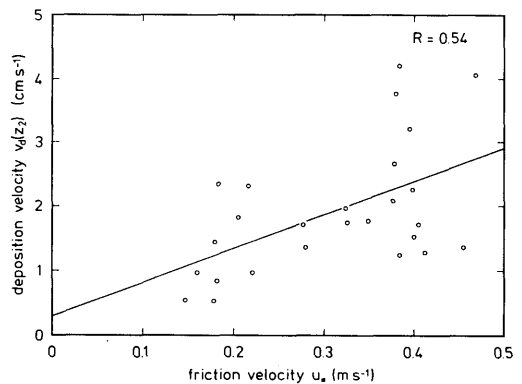


Fig. 12. Relationship between the deposition velocity derived for $z_2 = 3.83 \text{ m}$ and the calculated friction velocity (hourly averages), according to eq. (23). R is the correlation coefficient.

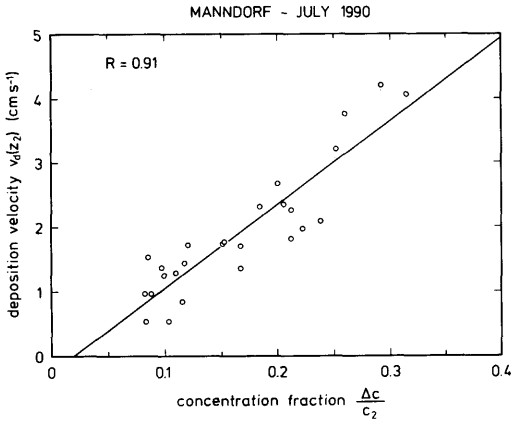


Fig. 13. Relationship between the deposition velocity derived for $z_2 = 3.83$ m and the concentration fraction (see eq. (10)). R is the correlation coefficient.

by $\Delta c/c_2$ and $\delta H/H$, where for $\delta v_d/v_d > 36\%$ the influence of $\Delta c/c_2$ is dominant. Note, however, that the large value of 63.3% is due to uncertainties in the $\delta\theta/\Delta\theta$ environment at nearly neutral conditions (see Table 3).

Taking eq. (10) into account, eq. (26) can be rearranged to

$$B_c^{-1} = u_* \left(r_{mt} + \frac{u_1}{u_*^2} \right), \quad (31)$$

where $r_{mt} = r_t((\Delta c/c_2)^{-1} - 1)$. Since also a relationship between u_1 and u_* exists with a satisfac-

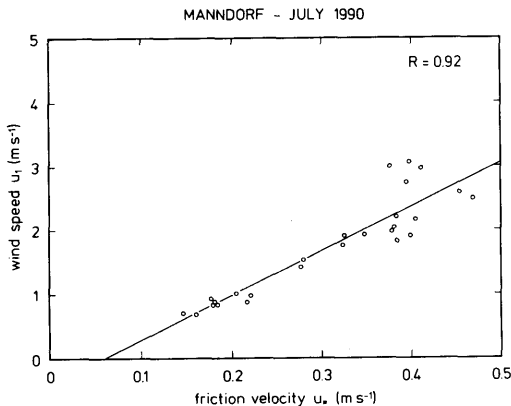


Fig. 14. Relationship between the measured wind speed $u_1 = u(z_1)$ and the calculated friction velocity (hourly averages). R is the correlation coefficient.

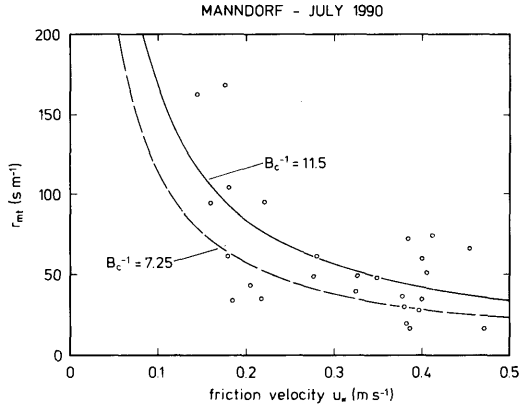


Fig. 15. Relationship between the molecular-turbulent resistance r_{mt} and the friction velocity (hourly averages). The solid line denotes the parameterization of r_{mt} (see eq. 24) with $B_c^{-1} = 11.5$ (this study), and the broken line that with $B_c^{-1} = 7.25$ (suggested by Hicks et al., 1987).

tory accuracy (see Fig. 14), the large scatter in the B_c^{-1} -values can be considered as a measure of the variability of $\Delta c/c_2$, too. This holds also for r_{mt} estimated by the *residuum method* (see Fig. 15).

4. Final remarks and conclusions

Based on 29 HNO₃ runs at Halvergate (grass, grazed pasture) and Manndorf (mature wheat), the average deposition velocity v_d was found to be 2.2 ± 1.2 cm s⁻¹ with a range of 0.6 to 5.0 cm s⁻¹. This agrees well with the results reported by Huebert and Robert (1985), Harrison et al. (1989), and Dollard et al. (1990).

Values of sublayer Stanton number B_c were deduced from eq. (26) assuming that deposition is determined mainly by atmospheric transfer. For the 26 continuous (1 h) Manndorf runs, B_c^{-1} ranged from 1.7 to 24.5 with a mean value of 11.5 ± 7.4 . The large scatter was shown to be mainly associated with variations in the concentration fraction $\Delta c/c$.

Values of B_c^{-1} obtained from the sublayer transfer relationship (29) are considerably larger than $B_c^{-1} = 7.25$ and those derived by the *residuum method* (eq. (26)). A reason for this is that B_c^{-1} (depending via the special Reynolds number Re_{*r} on the sublayer thickness z_r) has been calculated with $z_r = d + z_0$ indeed, but in doing so the values

of γ , m , and n (derived by Owen and Thomson (1963) for very special conditions) have been adopted unchanged. Therefore, the discrepancy to $B_c^{-1} = 7.25$ (proposed by Hicks et al., 1987) and to the residual values $B_c^{-1} = 11.5$ suggests that m , n , and in particular γ may be quite different for taller vegetation (see also Chamberlain, 1968).

Our results of deposition fluxes and velocities were derived via modified Bowen ratio and aerodynamic profile techniques which are based on the constant flux approach. This procedure is appropriate if in the absence of NH_3 the formation of HNO_3 acid by reaction (R4) is dominant. The linearity between the flux and the mean concentration as shown here might be considered as an indication that the influence of the chemical reactions was of minor importance during the field experiment at Manndorf.

Further HNO_3 formation by night-time chemistry (characterized by the $\text{NO}_3\text{-N}_2\text{O}_5\text{-HNO}_3$ cycle) and formation and depletion of HNO_3 by reactions (R5) and (R6) may generally produce height-dependent fluxes. In the case of transition between nitric acid and ammonium nitrate a dependence on height exists when the characteristic response time of this process is of several hundred seconds (see Figs. 3 and 4). Since, however, neither the reaction structure nor the reaction rate constants are well known, further research on this transition process is necessary to finally evaluate our (and previously published) results.

5. Acknowledgement

We should like to express our thanks to the Bundesminister für Forschung und Technologie, contracts 07EU713 7 and 07EU745 3, EUROTRAC-subproject BIATEX, Biosphere-Atmosphere Exchange of Pollutants, the Air Pollution Research Programme at Harwell funded by the Department of the Environment, contract PECD 7/12/5, and the Commission of the European Communities (COST 612), contract EV4V-0167-6 (GDF), for the support of these studies. Thanks also to the reviewers and Dr. Dennis D. Baldocchi for helpful comments and critical questions.

Appendix A

Following Kramm et al. (1991) and Kramm et al. (1993) the flux F_c at the interface *atmosphere-biosphere* can be parameterized for low horizontally uniform vegetation by (see Fig. 16)

$$F_c = \frac{c_s - H^*C_{\text{int}}}{r_{\text{st}} + H^*r_{\text{int}}} - \frac{1}{r_{\text{cu}}} (c_s - c_{\text{cu}}) - \frac{1}{H^*r_{\text{w,f}}} (c_s - H^*C_{\text{w,f}}) - \frac{1}{r_{\text{mt,g}} + r_{\text{sl,tot}}} \times \left(c_s - r_{\text{sl,tot}} \left(\frac{c_{\text{sl}}}{r_{\text{sl}}} + \frac{c_{\text{w,sl}}}{r_{\text{w,sl}}} \right) \right), \tag{A1}$$

with

$$r_{\text{st}} = \frac{r_{\text{st}}^*}{1 - \sigma_{\text{w,f}}}, \tag{A2}$$

$$r_{\text{int}} = \frac{r_{\text{int}}^*}{1 - \sigma_{\text{w,f}}}, \tag{A3}$$

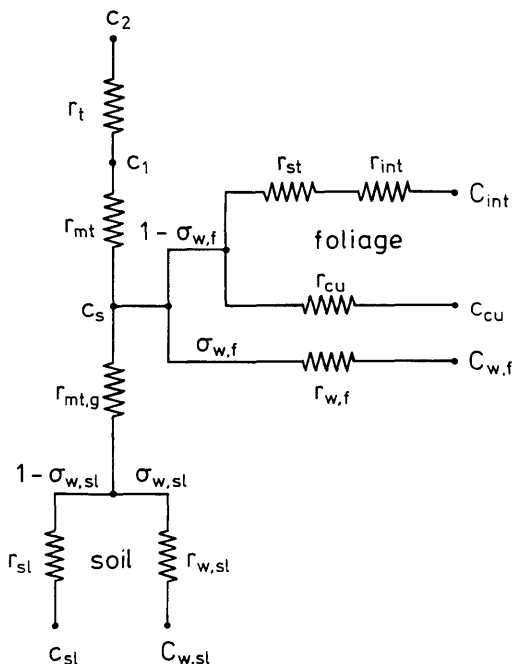


Fig. 16. Resistance network for the system vegetation-soil (with reference to Kramm et al. (1993)).

$$r_{cu} = \frac{r_{cu}^*}{1 - \sigma_{w,f}}, \tag{A4}$$

$$r_{w,f} = \frac{r_{w,f}^*}{\sigma_{w,f}}, \tag{A5}$$

$$r_{sl} = \frac{r_{sl}^*}{1 - \sigma_{w,sl}}, \tag{A6}$$

$$r_{w,sl} = \frac{r_{w,sl}^*}{\sigma_{w,sl}}, \tag{A7}$$

and

$$\frac{1}{r_{sl,tot}} = \frac{1}{r_{sl}} + \frac{1}{H^* r_{w,sl}}. \tag{A8}$$

Here, r_{st}^* is the stomata resistance, r_{int}^* is the internal resistance (see O'Dell et al., 1977), r_{cu}^* is the cuticular resistance, r_{sl}^* is the resistance of nearly dry soil, $r_{w,f}^*$ and $r_{w,sl}^*$ are the resistances of water (leaf wetness and soil water etc.), and $\sigma_{w,f}$ and $\sigma_{w,sl}$ ($0 \leq \sigma_w \leq 1$ for both cases) are wetness factors representing fractional foliage surface and fractional ground surface covered by water. The quantities C_{int} , c_{cu} , c_{sl} , $C_{w,f}$ and $C_{w,sl}$ are the substrate concentrations, where C_{int} , $C_{w,f}$ and $C_{w,sl}$ refer to aqueous solutions, and H^* is Henry's law constant for HNO₃.

The leaf resistances are bulk resistances. In the case of low vegetation they may be scaled according to the unit area of the ground surface (as a first approximation) by the leaf area index (LAI), i.e., $r_{st}^* = r_{st}^{**}/LAI$, $r_{int}^* = r_{int}^{**}/LAI$, $r_{cu}^* = r_{cu}^{**}/LAI$, and $r_{w,f}^* = r_{w,f}^{**}/LAI$, where r_{st}^{**} , r_{int}^{**} , r_{cu}^{**} , and $r_{w,f}^{**}$ are resistances expressed in terms of a unit area of foliage surface (see, e.g., Hicks et al., 1987; Hanson and Lindberg, 1991). The quantities r_{st}^{**} , r_{int}^{**} and r_{cu}^{**} are dependent on the species, where r_{st}^{**} is, in addition, a strong function of the photosynthetically active radiation (PAR). In the case of taller vegetation and tree canopies with highly varying leaf area density (which leads to varying sorption conditions), it appears to be necessary to divide the canopy layer into several foliage layers, where for each foliage layer a resistance network analogous to that shown in Fig. 16 can be used, and where the exchange between the adjoining foliage layers can be described on the basis of a molecular-turbulent resistance similar to $r_{mt,g}$, predominant for the exchange between the lowest

foliage layer and the ground (see also Baldocchi, 1988).

It may be assumed that in the case of HNO₃ deposition the quantities H^*C_{int} , c_{cu} , $H^*C_{w,f}$, and $r_{sl,tot}$ ($c_{sl}/r_{sl} + C_{w,sl}/r_{w,sl}$) are small in comparison with the surface concentration c_s . Therefore, the flux F_c may be estimated by

$$F_c = -\frac{c_s}{r_s}, \tag{A9}$$

where the (overall) surface resistance, r_s , is given by the relation

$$\frac{1}{r_s} = \frac{1}{r_{st} + H^* r_{int}} + \frac{1}{r_{cu}} + \frac{1}{H^* r_{w,f}} + \frac{1}{r_{mt,g} + r_{sl,tot}}. \tag{A10}$$

Appendix B

The molecular-turbulent resistance, r_{mt} , for the layer ranging from the surface to the height z_1 is given by

$$r_{mt} = \int_0^{z_1} \frac{dz}{D_c + K_h}. \tag{B1}$$

The integral expression can be split up to give

$$r_{mt} = \int_0^{z_r} \frac{dz}{D_c + K_h} + \int_{z_r}^{z_1} \frac{dz}{K_h}. \tag{B2}$$

Here, the first integral expression describes the diffusive transfer across the viscous sublayer of thickness z_r in the immediate vicinity of the receptor surface and the second integral expression characterizes the predominant turbulent transfer across the layer $z_r \leq z \leq z_1$. Since the influence of thermal stratification is negligible close to the surface, the eddy diffusivity of heat can be replaced by the eddy diffusivity of momentum for neutral conditions ($K_m = u_* \kappa z$), i.e.,

$$r_{mt} = \frac{1}{D_c} \int_0^{z_r} \frac{dz}{1 + K_m/D_c} + \int_{z_r}^{z_1} \frac{dz}{K_m} \tag{B3}$$

or

$$r_{\text{mt}} = \frac{1}{D_c} \int_0^{z_r} \frac{dz}{1 + \text{Sc} K_m/v} + \frac{u_1 - u_r}{u_*^2}. \quad (\text{B4})$$

Since the mean wind speed at the height z_r extrapolates to zero, the second term on the rhs. of eq. (B4) is nearly equal to u_1/u_*^2 . Furthermore, using the roughness Reynolds number, $\text{Re}_* =$

$u_* z/v$ as a dimensionless height, eq. (B4) can be rearranged to:

$$r_{\text{mt}} = \frac{u_1}{u_*^2} + \frac{\text{Sc}}{u_*} \int_0^{\text{Re}_{*r}} \frac{d \text{Re}_*}{1 + \text{Sc} K_m/v}. \quad (\text{B5})$$

Here, u_* is the height-invariant friction velocity derived for the layer $z_r \leq z \leq z_1$.

REFERENCES

- Baldocchi, D. 1988. A multi-layer model for estimating sulfur dioxide deposition to a deciduous oak forest canopy. *Atmos. Environ.* 22, 869–884.
- Biscoe, P. V., Clark, J. A., Gregson, K., McGowan, M., Monteith, J. L., and Scott, R. K. 1975. Barley and its environment. *J. Appl. Ecol.* 12, 227–257.
- Brost, R. A., Delany, A. C., and Huebert, B. J. 1988. Numerical modeling of concentrations and fluxes of HNO_3 , NH_3 , and NH_4NO_3 near the surface. *J. Geophys. Res.* 93, 7137–7152.
- Brutsaert, H. W. 1982. Exchange processes at the Earth-atmosphere interface. In: *Engineering meteorology* (ed. E. Plate). New York: Elsevier, 319–369.
- Businger, J. A. 1973. Turbulent transfer in the atmospheric surface layer. In: *Workshop on micrometeorology* (ed. D. A. Haugen). Boston: Amer. Meteor. Soc., 67–100.
- Businger, J. A. 1986. Evaluation of the accuracy with which dry deposition can be measured with current micrometeorological techniques. *J. Appl. Meteor.* 25, 1100–1124.
- Cadle, S. H., Countess, R. J., and Kelly, N. A. 1982. Nitric acid and ammonia in urban and rural locations. *Atmos. Environ.* 16, 2501–2506.
- Chamberlain, A. C. 1961. Aspects of travel and deposition of aerosol and vapour clouds. Harwell, Berkshire: A.E.R.E.-Report HP/R 1261 (RP/14).
- Chamberlain, A. C. 1968. Transport of gases to and from surfaces with bluff and wave-like roughness elements. *Quart. J. R. Met. Soc.* 94, 318–332.
- Dlugi, R., Meier, U., Paffrath, M., and Quenzel, H. 1989. Entstehung, Verhalten und Ablagerung von gas-, partikel- und tropfenförmigen Reaktionsprodukten. Final Report on *Untersuchungen zur Waldschadensforschung und Wirkung von Umweltschadstoffen*. Bayerisches Staatsministerium für Landesentwicklung und Umweltfragen, p. 52 (in German).
- Dollard, G. J., Jones, B. M. R., and Davies, T. J. 1990. *Dry deposition of HNO_3 and PAN*. Harwell, Oxfordshire: A.E.R.E.-Report R 13780.
- Ehhalt, D. H. and Drummond, J. W. 1982. The tropospheric cycle of NO_x . In: *Chemistry of the unpolluted and polluted troposphere* (ed. H. W. Georgii and W. Jaeschke). Dordrecht/Boston/London: D. Reidel, 219–251.
- Finlayson-Pitts, B. J. and Pitts Jr., J. N. 1986. *Atmospheric chemistry*. Chichester/New York/Brisbane/Toronto/Singapore: J. Wiley & Sons, p. 1098.
- Fowler, D. 1978. Dry deposition of SO_2 on agricultural crops. *Atmos. Environ.* 12, 369–373.
- Fowler, D. 1984. Transfer to terrestrial surfaces. *Phil. Trans. R. Soc. Lond.* B305, 281–297.
- Galbally, I. E. 1971. Ozone profiles and ozone fluxes in the atmospheric surface layer. *Quart. J. R. Met. Soc.* 97, 18–29.
- Hanson, P. J. and Lindberg, S. E. 1991. Dry deposition of reactive nitrogen compounds. A review of leaf, canopy and non-foliar measurements. *Atmos. Environ.* 25A, 1615–1634.
- Hargreaves, K. J., Fowler, D., Storeton-West, R. L., and Duyzer, J. H. 1992. The exchange of nitric oxide, nitrogen dioxide and ozone between pasture and the atmosphere. *Environ. Poll.* 75, 53–59.
- Harrison, R. M., Rapsomanikis, S., and Turnbull, A. 1989. Land-surface exchange in a chemically-reactive system; surface fluxes of HNO_3 , HCl and NH_3 . *Atmos. Environ.* 23, 1795–1800.
- Herbert, F. and Kramm, G. 1981. A discussion of approximate relations for transfer and deposition of trace constituents in the ABL. In: *Atmospheric trace constituents* (ed. F. Herbert). Braunschweig/Wiesbaden: Friedr. Vieweg & Sohn, 27–40.
- Hicks, B. B., Baldocchi, D. D., Meyers, T. P., Hosker, Jr., R. P., and Matt, D. R. 1987. A preliminary multiple resistance routine for deriving dry deposition velocities from measured quantities. *Water, Air, and Soil Pollut.* 36, 311–330.
- Hildemann, L. M., Russell, A. G., and Cass, G. R. 1984. Ammonia and nitric acid concentrations in equilibrium with atmospheric aerosols: Experiment versus theory. *Atmos. Environ.* 18, 1737–1750.
- Huebert, B. J. and Robert, C. H. 1985. The dry deposition of nitric acid to grass. *J. Geophys. Res.* 90 (D1), 2085–2090.

- Kramm, G. 1989a. A numerical method for determining the dry deposition of atmospheric trace gases. *Boundary-Layer Meteorol.* 48, 157–176.
- Kramm, G. 1989b. The estimation of the surface layer parameters from wind velocity, temperature and humidity profiles by least squares methods. *Boundary-Layer Meteorol.* 48, 315–327.
- Kramm, G., Müller, H., Fowler, D., Höfken, K. D., Meixner, F. X., and Schaller, E. 1991. A modified profile method for determining the vertical fluxes of NO, NO₂, ozone, and HNO₃ in the atmospheric surface layer. *J. Atmos. Chem.* 13, 265–288.
- Kramm, G., Beheng, K.-D., and Müller, H. 1992. Vertical transport of polydispersed aerosol particles in the atmospheric surface layer. In: *Precipitation scavenging and atmosphere-surface exchange processes*, Vol. 2, The Semonin Vol. (ed. S. E. Schwartz and W. G. N. Slinn). Washington/Philadelphia/London: Hemisphere Publ., 1125–1141.
- Kramm, G. 1992. Development and application of diagnostic models of the atmospheric boundary layer for determining the dry deposition of trace gases. *EUROTRAC Annual Report 1991, Part 4, BIATEX*. Garmisch-Partenkirchen: EUROTRAC-ISS, 267–284.
- Kramm, G., Dlugi, R., and Müller, H. 1993. On the determination of dry deposition fluxes of ozone, nitric oxide and nitrogen dioxide. *EUROTRAC Newsletter*, 11. Garmisch-Partenkirchen: EUROTRAC-ISS, 2–9.
- Larson, T. V. and Taylor, G. S. 1983. On the evaporation of ammonium nitrate aerosol. *Atmos. Environ.* 17, 2489–2495.
- McRae, G. J. and Russell, A. G. 1984. Dry deposition of nitrogen-containing species. In: *Deposition both wet and dry* (ed. B. B. Hicks). Boston/London: Butterworth Publ., 153–193.
- Meixner, F. X. and Schröder, P. 1991. Organizing a joint field experiment over low vegetation. *EUROTRAC Newsletter*, 7. Garmisch-Partenkirchen: EUROTRAC-ISS, 4–6.
- O'Dell, R. A., Taheri, M., and Kabel, R. L. 1977. A model for uptake of pollutants by vegetation. *J. Air Poll. Control Assoc.* 27, 1104–1109.
- Owen, P. R. and Thomson, W. R. 1963. Heat transfer across rough surfaces. *J. Fluid Mech.* 15, 321–334.
- Paulson, C. A. 1970. The mathematical representation of wind speed and temperature profiles in the unstable atmospheric surface layer. *J. Appl. Meteor.* 9, 857–861.
- Perrino, C., De Santis, F., and Febo, A. 1990. Criteria for the choice of a denuder sampling technique devoted to the measurement of atmospheric nitrous and nitric acids. *Atmos. Environ.* 24A, 617–626.
- Possanzini, M., Di Palo, V., and Masia, P. 1992. Evaluation of a denuder method for ambient NO₂ measurements at ppb levels. *Int. J. Environ. Anal. Chem.* 49, 139–147.
- Richardson, C. B. and Hightower, R. L. 1987. Evaporation of ammonium nitrate particles. *Atmos. Environ.* 21, 971–975.
- Schwartz, S. E. 1986. Mass-transport considerations pertinent to aqueous phase reactions of gases in liquid-water clouds. In: *Chemistry of multiphase atmospheric systems* (ed. W. Jaeschke). Berlin/Heidelberg/New York/Tokyo: Springer, 415–471.
- Stelson, A. W. and Seinfeld, J. H. 1982. Relative humidity and temperature dependence of the ammonium nitrate dissociation constant. *Atmos. Environ.* 16, 983–992.
- Wesely, M. L. 1989. Parameterization of surface resistances to gaseous dry deposition in regional-scale numerical models. *Atmos. Environ.* 23, 1293–1304.
- Whiteman, C. D., Allwine, K., Fritschen, L.-J., Orgill, M. M., and Simpson, J. R. 1989. Deep valley radiation and surface energy budget microclimates. Part II: Energy budget. *J. Appl. Meteor.* 28, 427–437.